



Economic feasibility of grid-connected PV–RO and PV–MVC small desalination units for remote areas in The United Arab Emirates — A comparative study

A.M. Helal*, S.A. Al Malek, E.M. Al Hammadi, H.A. Al-Thani

The National Energy and Water Research Center (NEWRC), Abu Dhabi Water and Electricity Authority (ADWEA),

PO Box 54111, Abu Dhabi, UAE

Tel. +971 2 694 7018; Fax: +971 2 642 8994; email: amhelal@adwea.gov.ae

Received 16 July 2008; Accepted 12 February 2009

ABSTRACT

This work presents a comparative study between grid-connected photovoltaic–mechanical vapor compression (PV–MVC) and photovoltaic–reverse osmosis (PV–RO) seawater desalination units with a desalted water capacity of 100 m³/d. The two systems are designed to provide water to isolated communities in remote areas in the United Arab Emirates. It is assumed here that transportation of water to those areas is difficult and costly while power from the national grid is available. In this design problem, environmental safety, suitability to demand, simplicity and energy efficiency represent desirable design requirements. Mathematical models are utilized to design the desalination units and produce a preliminary design of the PV array. However, the different design models are not given in this paper. Detailed cost calculations are performed for each one of the suggested systems to assess their feasibility and cost effectiveness. A sensitivity study of water cost to labor cost, cost of electricity, carbon dioxide emission tax and solar panels cost is presented here, together with the computed design characteristics of each one of the two systems. Based on the same cost conditions, the study shows that water cost per cubic meter from the grid connected PV–RO plant is only 51% of the water cost from the grid connected PV–MVC one. The RO plant produced water for a total cost of 3.7 \$/m³, while water cost from the MVC plant was 7.29 \$/m³.

Keywords: Hybrid; Vapor compression; MVC; Desalination; Solar; Photovoltaic; PV; Environmental; Reverse osmosis; RO

1. Introduction

The main objective of this work is to compare, on an economic basis, between two alternative designs of a small capacity, 100 m³/d seawater (SW) desalination unit, utilizing electricity from solar panels while being connected to the national power grid for power supply during night time and blackout hours. The solar panels

will provide electricity directly to the desalination plants as long as the energy of the incident solar radiation is above a minimum value. Below that value, electricity will be derived from the grid.

The unit will provide water to isolated communities in remote coastal arid areas in The United Arab Emirates (UAE) which, although having access to electricity from the grid, lack a fresh water supply due to the difficulty and high cost of transportation.

*Corresponding author.

Reverse osmosis (RO) and mechanical vapor compression (MVC) systems have many advantages that make them most suitable for the design of such small desalination units. These two systems have been considered for this study. Coastal arid areas in the UAE enjoy exceptionally high solar radiation most of the year, which encourages the idea of powering the two electric-driven systems suggested here with electric power from photovoltaic panels during sunshine hours while deriving power requirements by night from the national grid. In addition, there are environmental safety, compactness, mobility, suitability to demand, simplicity and energy efficiency representing desirable design features.

2. Literature review

Darwish [1] studied the performance and characteristics of the single effect MVC system using a simplified mathematical model. He studied the dependence of the process characteristics such as the specific heat transfer area of the evaporator/condenser and preheaters and the specific power consumption on the top brine temperature and the driving force for heat transfer across the evaporator/condenser tube wall. The author concluded that the specific heat transfer area of the evaporator/condenser and the specific power consumption decrease as the top brine temperature is increased. Again, he reported that the specific power consumption decreases at low temperature difference between the condensing vapor and the boiling brine outside the tubes while the specific heat transfer area of the evaporator/condenser increases.

Al-Juwayhel et al. [2] presented a number of mathematical models that describe the performance of different vapor compression systems applied for seawater desalting including the MVC process. In their work, the authors came up to the same conclusions reported earlier by Darwish [1]. Comparison of the MVC system with other thermal vapor compression systems is given in their article. Similarly, the same conclusions of Darwish [1] were obtained in a third study conducted by Ettouney et al. [3] following the same analysis methodology. In that work, a detailed model for the analysis of the MVC process was used. The paper presents useful information about practical values of the design parameters and operating variables of the single effect MVC systems.

In another study, Darwish et al. [4] presented a thermodynamic analysis of a MVC system where the vapor compressor is driven by a turbine. High pressure Freon vapors generated in a solar-heated boiler are allowed to expand into the turbine, thus exerting work to drive the compressor. The low pressure freon vapors are then condensed in a condenser/preheater where the latent heat released is utilized to pre-heat the feed

seawater to the evaporator. Condensed freon is pressurized through pumping back to the boiler.

The use of photovoltaic cells as a source of energy is a suitable choice to power an electrically driven desalination system in remote areas where the location enjoys high irradiance most of the year, especially when the plant location is far away from the power grid. The possible use of single- or dual-axis trackers makes the array point directly at the sun throughout the day, which increases the amount of water produced by up to 30% [5]. Meanwhile, RO technology is becoming more popular as it is characterized by significantly low specific energy consumption, which is mainly dependent on water salinity, 3–9.4 kWh/m³ product [6].

Hafez and El-Manharawy [7] presented a detailed cost analysis of grid connected small RO plants built at tourist resorts in Sinai and Hurgada on the Red Sea coasts in Egypt. Capacities of the studied plants varied between 250 and 4800 m³/d. Production cost from the different plants showed inverse proportionality with plant capacity where the cost varied between 2.23 US\$/m³ for the 250 m³/d plant and 1.14 US\$/m³ for the 4800 m³/d plant.

So far, water cost from very small PV–RO units remains much higher than the cost per cubic meter of fresh water produced by conventional (large-capacity (>5000 m³/d), grid-connected) RO plants and the gap between the two costs has to be narrowed. Recent innovations in the solar panels manufacturing technology developed by Honda-2005 [8] and the continual research efforts done to increase their energy conversion efficiency will result in significant reduction in solar panels cost. This cost reduction will lead directly to reduction in water cost from solar-driven small RO units since panels cost represents a major item in the plant investment.

Fiorenza et al. [9] conducted a techno-economic study to explore the feasibility of utilizing solar energy for powering small to medium, grid-supported, desalination plants. In their study special attention has been paid to two main options, namely PV–RO and solar thermal multi-effect evaporation (ST–MEE). They tried to single out the factors to be investigated to fill the gap between solar and conventional technology production cost and examine other critical aspects of the solar technologies such as the required land area and amount of the initial investment

Al Suleimani et al. [10] reported an average water cost of 6.52 US\$/m³ for a demonstration PV–RO desalination unit with a battery backup and freshwater capacity of 5–7.5 m³/d which is produced during peak solar hours (5 h). The unit was built to desalinate brackish water at the Heelat ar Rakah camp, a remote location about 900 km south of Muscat, the capital of Oman. The authors claim that the demonstration PV–RO unit proved its adequacy

for remote locations that have limited or no access to fresh water, power and fuel services.

Thomson et al. [11] presented a cost effective battery-less photovoltaic powered RO desalination system with a water cost of 2 pounds sterling (3.64 US\$) per cubic meter. The plant capacity is 3 m³/d and the system has a modest 2.4 kWp PV array. The simple control system of the unit provides maximum power point tracking for the PV array. A full-cost analysis of the demonstration unit is given by Dulas and Machyn-lleth, UK [12]. In this cost analysis, estimations were based on a 20-year lifetime of the system as a whole, with pump replacement at 5, 10 and 15 years. An 8% discount rate was assumed and all membranes to be replaced every 12 months.

Another successful example is the Lampedusa autonomous PV-RO seawater desalination plant [13] commissioned in 1990. The plant was built and sized for demonstration purposes. It is capable of supplying 120 m³/d of desalinated water for 8 h of operation at a full load over three consecutive—but not necessarily sunny—days. The plant, powered by a system of 100 kW PV arrays, batteries and inverters, consists of an RO unit subdivided into two sections with respective product water capacities of 3 m³/h and 2 m³/h. Spiral-wound permeators are used in both sections. The power supply system is a 100 kWh PV array; batteries with storage capacity of 2×2,000 ampere-h (Ah) at 220 volts (V) DC are used. The inverters, one for each section, are sized to allow the 22 kW motors to start easily.

3. Characteristics and process description of the PV-MVC and PV-RO plants

3.1. PV-MVC process characteristics

Fig. 1 illustrates the process flowsheet of the single effect MVC plant and Fig. 2 shows a cross section in its evaporator shell. The MVC evaporator has many advantages including:

- Compactness and minimal requirement of ground area.
- The plant can be based on package design concept which makes it easy to dismantle, package and transport.
- Low energy requirements.
- No need for additional heating, e.g. boiler or electric heater.
- Ease of operation and maintenance.
- High reliability and robustness qualify the MVC plant to be used on offshore platforms.
- Suitability for small capacity of freshwater to meet requirements of small communities.
- Limited intake facilities.
- Favorable heat transfer characteristics.

- Evaporation takes place at a reduced temperature which minimizes corrosion hazard and scale formation.
- Simple chemical pretreatment equipment (not discussed here).

The design philosophy of the MVC plant presented here is to satisfy the requirements of compactness, simplicity, energy efficiency and environmental safety. For this purpose, the choice of a spray-type horizontal tube evaporator and recovery of heat energy through the use of plate exchangers both realize energy efficiency, heat transfer enhancement and compactness. Selection of titanium for tube materials and exchanger plates and passivated stainless steel for the evaporator shell combats corrosion and improves plant economics. The absence of a de-aerator and operation of the evaporator at a low brine temperature minimizes scale and corrosion hazard and eliminates the need for skilled labor to conduct acid cleaning while a simple acid dosing system can be used. However, the penalty is a relatively lower heat transfer coefficient, the need for a vacuum system and handling larger vapor volumes by the compressor which would require a more expensive compressor.

Another important point regarding material selection is that the extra cost of titanium tubes over copper-nickel is balanced by the use of thinner titanium tubes and exchanger plates. Titanium is also less dense than copper alloys and more resistant to corrosion attack. The use of a grid-connected PV power system reduces air pollution and helps the reduction of green house effect, saves atmospheric oxygen and reduces operation and maintenance costs.

3.2. PV-MVC process description

Fig. 1 represents the MVC desalination plant flowsheet. Fresh seawater feed at a flowrate \dot{m}_{F0} and a temperature T_{F0} is introduced to the plant by means of the feed pump where it is split up into two portions: The first portion, having a mass rate, \dot{m}_{F1} , goes into the tubes of the vent condenser to recover the latent heat of evaporation released by the vapors that escaped condensation at the evaporator/condenser and which are condensing outside the vent condenser tubes. This heat recovery process will bring the seawater stream temperature up to a value of T_{F1} . The warm seawater leaving the vent condenser is further heated up to a temperature T_{F3} in a subsequent heat recovery process by exchanging heat with the hot blowdown stream leaving the evaporator at a mass flowrate \dot{m}_B and a temperature T_{B1} . This heat recovery process takes place in a plate exchanger, *HX2*.

The second portion, having a mass rate \dot{m}_{F2} , is pre-heated to a temperature T_{F2} by exchanging heat with the

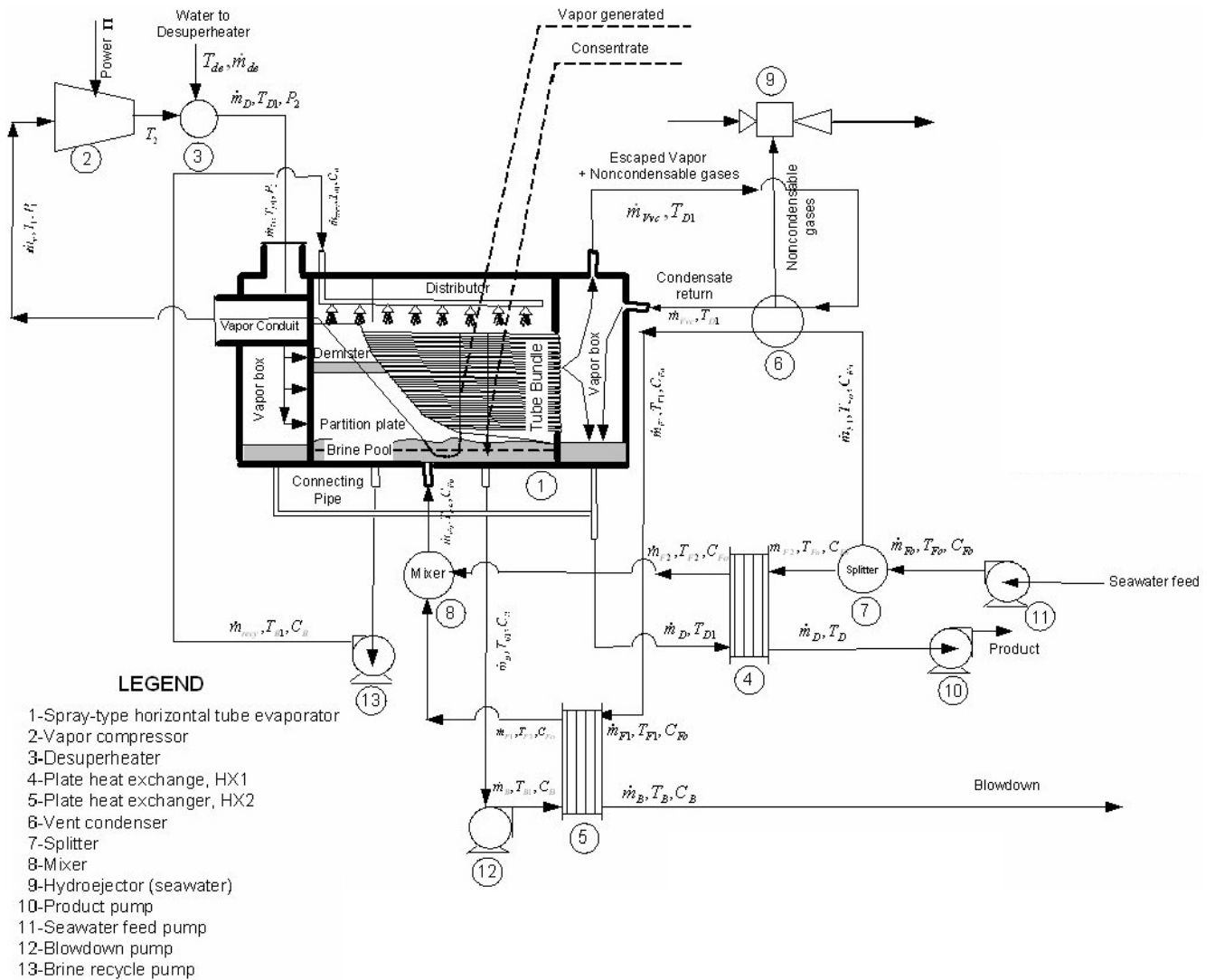


Fig. 1. MVC plant. Process flow sheet with longitudinal section of the evaporator.

hot distillate leaving the evaporator vapor box at a rate \dot{m}_D and a temperature T_{D1} in a second plate exchanger, HX1. Preheated seawater streams at T_{F2} and T_{F3} leaving heat exchangers are then mixed together and the combined stream at T_{F4} is passed to the brine pool inside evaporator shell.

A recycle pump takes its feed from the brine pool at the bottom part of the evaporator shell. The recycled brine at a rate \dot{m}_{recy} is introduced to the brine distribution headers and sprayed, through spray nozzles, to form a thin film over the outside surface of two tube banks laid horizontally in two separate compartments. Evaporation takes place at T_{B1} on the hot tube surface, which is receiving the latent heat of the compressed vapors condensing inside the tubes at a temperature T_{D1} . Both vapor and concentrated brine with the flow rates \dot{m}_V and \dot{m}_{con} respectively will move downwards across the tube

bundle towards the brine pool surface. The vapor generated is then deflected by 180 degrees around the lower edge of a partition plate, detached from the accompanying brine and then passes through the demisters for mist elimination, then to a vapor conduit leading to suction point of the vapor compressor.

The vacuum system reduces the pressure inside the evaporator to a value of $P = 15.73$ kPa which corresponds to a saturation temperature, T_s of about 55°C while evaporation takes place on the tube surface at a temperature $T_{B1} = (T_s + \Delta BPR)$ where ΔBPR represents the boiling point rise.

Passing through the compressor, the vapor pressure is increased to a value of 19.1 kPa. This pressure corresponds to a saturation temperature, T_{D1} (after de-superheating and allowance for pressure drop from compressor exit to evaporator tubes). Thus, the net driving force for heat

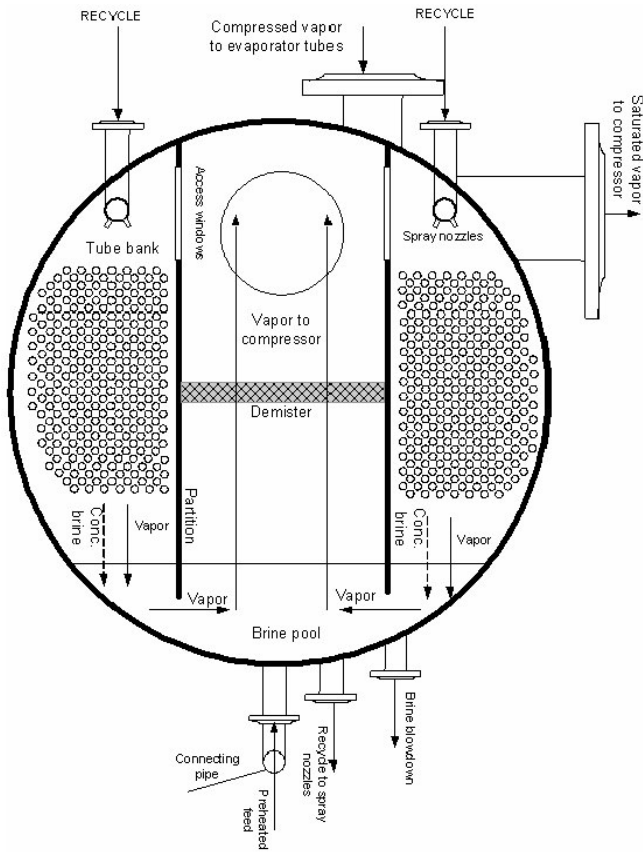


Fig. 2. Cross section in the evaporator shell.

transfer across the tube walls is $(T_{D1} - T_{B1})$. After de-superheating, the compressed vapor flows to the vapor box at one end of the evaporator. From there it is distributed on all the tube inlets. Moving towards the other end, most of the vapor is condensed. This way, the latent heat released is transferred to the thin film of brine surrounding the outside tube surfaces where evaporation takes place. The mixture composed of uncondensed vapor, condensate and non-condensable gases leaves the other tube end to a second vapor box where the remaining vapor is condensed in the vent condenser and returned back to join the distillate in the vapor box. At the vent condenser, small amount of the vapor and the non-condensable gases are sucked by the seawater hydro-ejector, and mixed with the ejecting seawater stream. Non-condensable gases are discharged to the atmosphere. Ejecting brine is recycled by means of a second recycle pump, which is a part of the vacuum system, (details of ejecting system are not shown). The two vapor boxes at the opposite ends of the evaporator are connected by a tube for pressure equalization. A distillate pump connected to that tube moves the combined distillate to the fresh water storage tank. A cross section of the evaporator shell showing its details is depicted in Fig. 2.

Start-up of the evaporation process requires vacuum generation. The compressor is first run at a small RPM thus handling a very small vapor flow rate. The speed is increased slowly for about 2–3 h. Through the compressor, the air in the plant is compressed and passes a little heat to the tubes. Part of the air is extracted by the air suction unit (water ejector). If the seawater inflow is then activated, this heat causes a small part of the seawater to evaporate, which then passes into the compressor cycle. On compression, air temperature is increased then heat is again transferred, and this time it is a little more. The air suction unit continues to extract more and more air from the plant until the operation has established. This way, the air suction unit indirectly controls the duration of the start-up procedure. As soon as the partial pressure of the vapor component exceeds the vapor pressure at the saturation temperature inside the evaporator/condenser tubes, the vapor condenses suddenly and the process is thus brought to steady state operation.

3.3. PV-RO process characteristics

RO technology is becoming more popular because of the following advantages:

- The specific energy requirement is significantly low
- The process is electrically driven. As a result, it is readily adaptable to powering by solar panels.
- The RO plant is normally operated at ambient temperature, which reduces the headache of scale formation and corrosion problems, especially when the pretreatment system is properly designed and kept under control. Again this will reduce maintenance cost.
- The modular structure of the RO process increases flexibility in building desalination plants within a wide range of capacities.

3.4. PV-RO process description

A simplified flowsheet for the RO plant studied here is shown in Fig. 3. The plant has two stages where seawater is pumped to the pretreatment section by means of the intake pump. Pretreated seawater flows to the high pressure pump where its pressure is increased to a value between 55 and 80 bars before it is introduced to the permeators of the first stage. The relatively high pressure reject from stage 1 is directed to the energy recovery device, assumed to be a pressure exchanger, and then discharged to the outfall. The permeate leaving stage 1 at atmospheric pressure is then pressurized by a booster pump to a pressure between 15 and 40 bars to be desalinated further in stage 2. Permeate leaving the second stage will have a level of TDS below 500 ppm and the reject is discharged into the outfall.

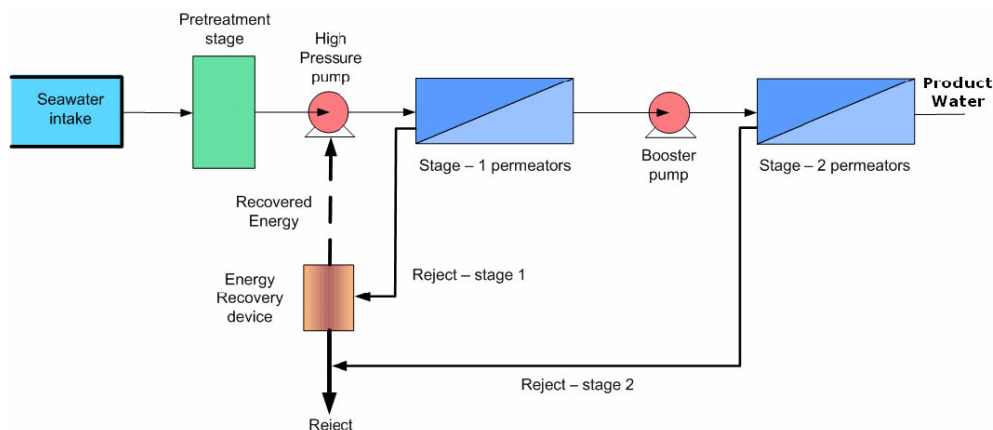


Fig. 3. Simplified RO desalination plant flow sheet.

Filmtec FT30 SW2.5" seawater membranes are used in stage 1 while brackish water Filmtec BW 2.5" membranes are used in stage 2. Two spiral-wound membranes per pressure vessel were selected for this study. Details of the pre- and post-treatment stages are not given here.

The choice of a two-stage plant was based on the assumption that a single stage RO unit would be adequate to produce the required salinity of potable water, 500 ppm or less, when brackish water is fed to the membranes. For highly concentrated seawater like the Gulf water, a two-stage plant would be more preferable, since a single-stage plant with high salt rejection membranes would result in increased effect of concentration polarization, which in turn will reduce the net driving force and consequently reduce permeate flux.

In this work, it is assumed that both plants, the RO and MVC plants, will be equipped with a 300 m³ capacity tank, a storage capacity which is believed to be enough for backing up the system for 3 days allowing for unreliable weather conditions, unplanned system downtime and variability in consumption.

4. Mathematical modelling

4.1. MVC plant — design model

Helal et al. [14] give full details of the mathematical model for the design of all equipment comprising the single-effect MVC system described here. As seen from the plant flow sheet, the main equipment includes: evaporator, vapor compressor, plate heat exchangers and vent condenser.

4.2. RO plant — design model

For the design purpose of the RO plant, the simplified model developed by Avlonitis et al. [15] has been used. In

spite of the simplicity of the model's equations, geometric details of the spiral wound membrane have been taken into account. Such details include number of leaves (in this work, one leaf membranes are used), membrane length and width and height of brine and permeate channels. Other factors have been accounted for such as pressure drop in permeate and brine channel, concentration polarization and concentration gradient along the module.

However, in their derivation, the authors assumed ideal conditions for the feed solution and the membrane performance. All the effects of fouling, scaling, chemical deterioration of membranes have been ignored. To counterbalance the last assumption, a fouling factor of 0.7 has been used here to augment the permeate flux equation. The simple formulation of the model's equations enabled a straightforward solution procedure although being iterative in nature.

4.3. Solar array design model

Design of the solar array is based on the radiation data of Abu Dhabi, UAE. The list of equations used for the preliminary design of the array can be found in Markvart [16].

4.4. Carbon dioxide emission calculations

These calculations are simple and straightforward. Details of the mathematical expressions used in these calculations can be found elsewhere [14].

Although neither of the two plants burns fuel at the plant site, the electric power derived from the grid to keep these plants running during nighttime and black-out hours, necessitates burning a certain amount of fuel at the power plant, thus releasing a proportional amount of carbon dioxide.

4.5. Cost model

For the RO plant calculations, the capital cost equations used in this work are derived from Marcoveccio et al. [17]. The same equations were used by Helal et al. [18] to study the economic feasibility of small capacity RO plants with alternative powering systems, namely hybrid PV–diesel powered, solar PV powered and diesel powered. It is noteworthy to mention that no cost data on small capacity MVC were found throughout the available literature. The equipment costs of the MVC system used for calculations in this work are taken from the purchasing documents of a similar system built for ADWEA in 1997. Costs have been updated for 2007 using the Marshall and Swift index.

It would be useful to know that the cost of electricity for industrial purposes in the UAE is equivalent to 4 US cent/per kWh. In this study, a figure of 3 US cent/per kWh has been used, assuming that a reduction of 25% of electric energy cost can be given to the consumers in order to encourage renewable energy utilization.

5. Results and discussion

The design of the MVC plant is optimized based on an objective of minimum total sum of heat transfer areas of the evaporator, two plate exchangers and vent condenser. The objective function is subject to the following constraints:

- 0.15 m < width of plates < 0.5 m
- 1 < plate height < 1.5 m
- 1 < clean coefficients of heat transfer in exchangers, evaporator and condenser exchanger < 4.5 kW/m² k
- All model equations to be satisfied

At the same time, the RO plant design is subject to the following conditions:

- 55 bar < feed pressure to stage 1 < 80 bar
- 15 bar < feed pressure to stage 2 < 30 bar
- 32% < recovery of stage 1 < 37 %
- 80% < recovery of stage 2 < 90%
- Water flux across permeators < 25 Imperial gal/m²/d
- Final product concentration < 500 ppm
- All model equations to be satisfied

Input data for the two plants are listed in Tables 1–6. Table 1 gives the input for the MVC plant components and Table 2 includes the data for the solar powering system.

Tables 3 and 4 present the data input for the RO plant and its pumping and energy recovery equipment.

Design characteristics calculated for the MVC system are given in Tables 7 and 8. Similarly, characteristics of the RO plant are given in Table 9.

Table 1

Input data—MVC desalination plant (reference data set)

| General | |
|--|----------|
| Plant capacity, m ³ /d | 100 |
| Recovery ratio (MVC-distillate to feed ratio) | 0.45 |
| Seawater temperature, °C | 20 |
| Seawater concentration, ppm | 45,000 |
| Evaporator | |
| Condensation temperature inside tubes, °C | 59.00 |
| Brine pool temperature, °C | 55.94 |
| Average boiling point rise in brine pool | 0.94 |
| Nonequilibrium loss | 0 |
| Tube material | Titanium |
| Demister thickness, m | 0.1 |
| Outside diameter of tubes, m | 0.03 |
| Tube thickness, m | 0.0005 |
| Tube length, m | 5 |
| Thermal conductivity for Ti tubes, kW/mK | 0.038 |
| Fouling factor, m ² K/kW | 0.11 |
| Spray density, kg/ms | 0.08 |
| Condensate discharge angle, ° | 45 |
| Angle of circumference, ° | 135 |
| Sat. temp. difference across evaporator tubes, °C | 3.5 |
| Vapor compressor | |
| Mechanical efficiency | 0.75 |
| Motor efficiency | 0.78 |
| Adiabatic compressibility factor - gamma | 1.34 |
| Temperature of water to desuperheater, °C | 25 |
| Plate heat exchangers 1 and 2 | |
| Fouling factor, m ² K/kW | 0.10 |
| Thermal conductivity of plate material, kW/mK | 0.038 |
| Plate thickness, m | 0.002 |
| Vent condenser | |
| Fouling factor, m ² K/kW | 0.10 |
| Thermal conductivity of tube material, kW/m.K | 0.038 |
| Tube thickness, m | 0.0005 |
| Inside tube diameter, m | 0.0125 |
| Uncondensed rate of vapor to vent condenser (2% of distillate), kg/h | 82.9 |
| Linear velocity of cooling seawater, m/s | 1.80 |
| Number of tube passes | 1 |
| Percent noncondensable gases in feed | 0.05 |
| Temp. rise of seawater within vent condenser, °C | 8 |

Design characteristics calculated for the MVC system are given in Tables 7 and 8. Similarly, characteristics of the RO plant are given in Table 9, and the design features of the solar powering systems for the two plants are given in Tables 10 and 11.

From the values given in Table 12 for water cost from the two plants, it is found that the PV–RO plant is much more economically feasible than the PV–MVC plant where, for the given design conditions, water cost from the former is only 59% of the cost calculated for the latter (3.7 \$/m³ for the RO vs. 7.29 \$/m³ for the MVC system).

Table 2

Module characteristics: input data for the solar powering system (reference data set)

| Type | Total Energie TE850A2 |
|---|--------------------------|
| Nominal voltage, V | 12.00 |
| Nominal current (short circuit current), A | 5.20 |
| Number of cells | 36.000 |
| Area/cell, m ² /cell | 0.016 |
| Area of module, m ² | 0.563 |
| Efficiency deterioration | 0.2 |
| Number of peak solar hours in plant location, h | 16.4 |
| Daylight hours, h | 10.8 |
| Inverter efficiency | 0.9 |

Table 3

Membrane characteristics: input data for RO plant (reference data set)

| | Stage 1 | Stage 2 |
|--|----------------------------|--------------------|
| | Filmtec FT30 SW 2.5" | Filmtec BW 2.5" |
| Water permeability coefficient, m.S ⁻¹ Pa ⁻¹ | 0 | 4.70E-12 |
| Salt permeability coefficient, m/s | 3.34E-07 | 2.52E-07 |
| Mass transfer coefficient, m/s | 3.68E-05 | 3.68E-05 |
| No. permeators/PV in stage 1 | 2 | |
| Atmospheric pressure, Pa | 1.00E+05 | |
| Modular length (without glue), m | 0.867 | |
| Modular width (without glue), m | 1.17 | |
| Membrane area, m ² | 2.02878 | |
| Height of permeate channel, m | 0.00043 | |
| Height of brine channel, m | 0.00077 | |
| Dissociation factor | 0.9 | |
| Number of ions resulting on dissociation | 2 | |
| Gas constant, m ³ .atm/g mole.K | 0.00008206 | |
| Molar density of water, kmol/m ³ | 55.56 | |
| Salt molecular weight, kg/kg mole | 58.5 | |
| Friction parameter (permeate), m ⁻² | 1.10E+09 | |
| Solution viscosity, kg/ms | 0.00089 | |
| Solution density, kg/m ³ | 1100 | |
| Diffusivity, m ² /s | 1.60E-09 | |
| T20, °C | 20 | |

Table 4

Input data for RO plant — pumps and energy recovery (reference data set)

| | |
|--|-----|
| Pump motor efficiency | 0.8 |
| Mechanical efficiency of pumps | 0.8 |
| Intake pump, assumed exit pressure, bar | 4 |
| Product pump, assumed exit pressure, bar | 4 |
| Energy recovery efficiency | 0.9 |

Table 5

Input data: cost data for MVC and RO plants (reference data set)

| | |
|--|--------------------|
| Cost of land, US \$/m ² | 50 |
| Site development | 25% of DCC |
| Indirect CC_ contingency | 10% of DCC |
| Capital recovery period, y | 25 |
| Interest rate, % | 5 |
| Installation cost | 20% of equip. cost |
| CO ₂ tax, US \$/ton | 31.75 |
| Installed cost for storage tank, \$/m ³ | 300 |
| Storage tank capacity, m ³ | 300 |
| Labor cost (3 laborers×1500 \$/month ×12 month/y), \$/y | 54,000 |
| Electricity cost, \$/kWh | 0.03 |
| Installed cost of solar panels, \$/We | 8.17 |
| MVC equipment cost (CIF) (purchase invoices), \$ | 1,111,153 |
| MVC, installed pretreatment and intake cost, \$/m ³ (feed) | 200 |
| MVC, spares cost, \$/m ³ (product) | 0.082 |
| MVC, chemicals cost, \$/m ³ (product) | 0.024 |
| RO/stage 1 membrane element cost \$/element | 194 |
| RO/stage 2 membrane element cost \$/element | 172 |
| RO, installed pretreatment and intake cost [996×(Q _f) ^{0.8}] ^a , \$ | 107,335.99 |
| RO, spares cost, \$/m ³ (product) | 0.033 |
| RO, chemicals cost, \$/m ³ (feed) | 0.018 |

^aQ_f = feed rate.

Table 6

Input data for power plant and fuel characteristics (for CO₂ emission calculations)

| | |
|---|-------------|
| Overall power plant efficiency (heat to electricity), % | 35 |
| Fuel | Natural gas |
| Fuel density, kg/m ³ at STP | 0.65 |
| Calorific value of natural gas, GJ/kg | 0.054 |
| Mass fraction carbon in fuel | 0.75 |

Table 7
Output data for the MVC desalination plant

| | |
|---|----------|
| Evaporator | |
| Tube material | Titanium |
| Thermal conductivity of tube material, kW/mK | 0.0380 |
| Outside tube diameter, m | 0.03 |
| Tube thickness, m | 0.0005 |
| Tube length, m | 5.0 |
| Number of tubes | 585 |
| Vapor space pressure, kPa | 15.7 |
| Vapor space temperature, °C | 55.00 |
| Spray density, kg/s.m length | 0.08 |
| Temp. difference across tubes, °C | 3.50 |
| Overall heat transfer coefficient, clean operation, kW/m ² K | 3.98 |
| Fouling factor, 1/(kW/m ² K) | 0.11 |
| Inside shell diameter (cylindrical), m | 2.0 |
| Vapor compressor | |
| Suction pressure, kPa | 15.60 |
| Suction temperature, °C | 54.83 |
| Compression ratio | 3.50 |
| Discharge temperature before desuperheater, °C | 70.07 |
| Mechanical efficiency | 0.75 |
| Motor efficiency | 0.78 |
| Power rating, kW | 56.32 |

Table 9
Output data for RO plant design

| | |
|---|----------|
| Plant recovery, % | 29 |
| Stage 1 recovery R1, % | 32.00 |
| Stage 2 recovery R2, % | 90.00 |
| No. of pressure vessels, Stage 1 ^a | 28 |
| No. of pressure vessels, Stage 2 ^a | 26 |
| Total membrane area, m ² | 213.39 |
| Feed pressure to stage 1, Pa | 5.50E+06 |
| Feed pressure to stage 2, Pa | 1.54E+06 |
| Final product concentration, ppm | 144 |

^aTwo membranes in each pressure vessel.

Table 10
Output data for the solar PV array design, MVC desalination plant

| | |
|---|--------|
| Output AC power required, kW(AC) | 65.22 |
| No. of modules (desal plant array) | 928.00 |
| No. modules in a series line | 32.00 |
| Number of parallel lines | 29.00 |
| DC voltage, V | 384.00 |
| Load current, A | 228.30 |
| Maximum DC power output from PV array, kW(DC) | 87.67 |
| Maximum AC power output from inverter, kW(AC) | 78.90 |
| Total area of modules, m ² | 522.00 |

Table 8
Output data for the MVC desalination plant (continued)

| | |
|--|----------|
| Plate heat exchanger 1 | |
| Plate material | Titanium |
| Thermal conductivity of plate material, kW/mK | 0.0380 |
| Plate width, m | 0.22 |
| Plate length, m | 1.27 |
| Plate thickness, m | 0.0020 |
| Gap between plates, m | 0.004 |
| Number of plates | 102 |
| Log mean temp. difference, °C | 1.0 |
| Fouling factor, 1/(kW/m ² K) | 0.10 |
| Overall heat transfer coefficient, clean operation kW/m ² K | 4.5 |
| Plate heat exchanger 2 | |
| Plate material | Titanium |
| Thermal conductivity of plate material, kW/mK | 0.0380 |
| Plate width, m | 0.26 |
| Plate length, m | 1.50 |
| Plate thickness, m | 0.0020 |
| Gap between plates, m | 0.004 |
| Number of plates | 112 |
| Log mean temp. difference, °C | 3.1 |
| Fouling factor, 1/(kW/m ² K) | 0.10 |
| Overall heat transfer coefficient, clean operation kW/m ² K | 1.1 |
| Vent condenser | |
| Tube material | Titanium |
| Thermal conductivity of tube material, kW/mK | 0.0380 |
| Tube length, m | 1.53 |
| Inside diameter of tubes, m | 0.0125 |
| Tube thickness, m | 0.0005 |
| No. of U-shaped tubes | 8 |
| Log mean temp. difference, °C | 34.3 |
| Overall heat transfer coefficient, clean operation kW/m ² K | 4.4 |
| Fouling factor, 1/(kW/m ² K) | 0.10 |

Table 11
Output data for solar PV array design, RO plant

| | |
|--|--------|
| Output AC power required (energy rec.), kW(AC) | 26.87 |
| No. of modules | 400.00 |
| No. of modules in a series line | 20.00 |
| No. of parallel lines | 20.00 |
| DC voltage, V | 240 |
| Load current, A | 124.41 |
| Max. DC power available from RO array, kW(DC) | 37.49 |
| Max. AC power available from inverter, kW(AC) | 26.87 |
| Total area of modules, m ² | 225.20 |
| Actual DC power required, kW | 29.86 |

Table 12

Output data for water cost and its sensitivity to changes in operational costs

| | | |
|---|--------|------|
| Product cost, \$/m ³ | PV-MVC | 7.29 |
| | PV-RO | 3.7 |
| Sensitivity to labor cost (cent/m ³)/\$100 (increase in monthly salary) | PV-MVC | 11.8 |
| | PV-RO | 11.6 |
| Sensitivity to electrical cost (cent/m ³)/(cent/kWh) | PV-MVC | 8.96 |
| | PV-RO | 3.70 |
| Sensitivity to CO ₂ emission tax (cent/m ³)/(\$/ton) | PV-MVC | 0.47 |
| | PV-RO | 0.19 |
| Sensitivity to installed panels cost (cent/m ³)/(\$/We) | PV-MVC | 11 |
| | PV-RO | 5 |

Results concerning the net AC power requirements for the MVC and RO systems studied here confirm the known fact that the MVC process consumes more energy per cubic meter of product than the RO process. From the figures given in Tables 10 and 11, the net AC power ratings are 65.22 kW for the MVC plant against 26.87 kW for the RO plant. This is equivalent to 15.7 kWh/m³ for the MVC plant and 6.45 kWh/m³ for the RO plant. Specific energy consumption for the RO plant lies well within the known range of specific energy consumption normally reported in literature, 3–9.4 kWh/m³. However, it is known that the power requirements of the compressor at the MVC plant depend to a great extent on the saturation temperature difference across the condenser/evaporator tube surface as well as the brine pool temperature. Depending on the saturation temperature difference across the evaporator tube wall and the top brine temperature, values between 6 and 19 kWh/m³ are reported in the literature for the MVC process [1–3,19]. The smaller the temperature difference across the evaporator tube wall and the higher the top brine temperature, the lower the specific power consumption. The relatively high value of 15.7 kWh/m³ obtained in this work is a result of selecting a saturation temperature difference of 3.5°C across the tubes to ensure a reasonable driving force for heat transfer and to end up with an evaporator design with less heat transfer area and less capital cost. This issue was discussed in more detail by Helal et al. [14].

In general, power requirements have a direct bearing on the number of PV modules and the installed costs of the solar powering system of each plant. The effect extends to the land area required and ultimately to the product cost. These facts are clear from the results obtained and listed in Tables 9 and 10 where for the RO plant, the total power required is only 26.87 kW, while for the MVC plant it goes up to 65.2 kW. Accordingly, the number of PV modules is 400 for the RO plant with a total module area of 225 m² while the corresponding figures for the MVC plant are; 928 modules and 522 m² respectively.

Table 12 outlines the sensitivity of product water cost to variations in some operational costs, namely; labor cost, electricity cost, CO₂ emission tax and installed cost of solar panels. Each one of these operating costs was varied over a certain range, as shown in Figs. 4–7. These figures show that water cost from both plants assumes a linear trend over the selected range of the cost element shown on the x-axis.

As has been shown above, the MVC technology requires more electric energy consumption per unit product than the RO technology. As a result, it would be



Fig. 4. Effect of labor cost on water cost.

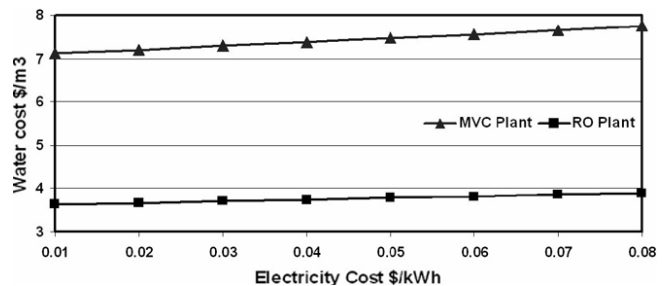


Fig. 5. Effect of electricity cost on water cost.

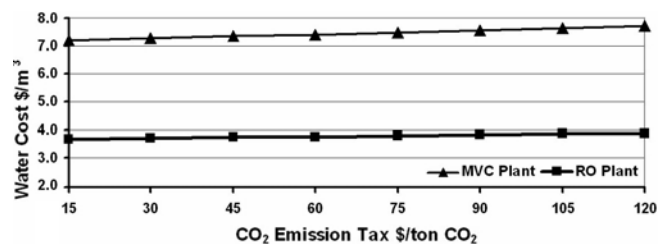
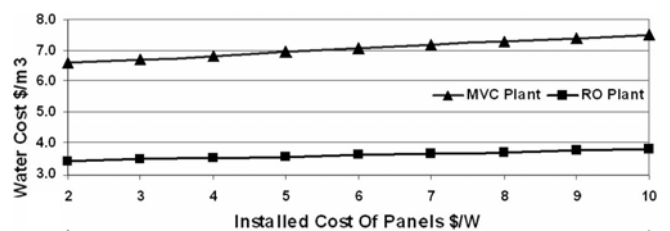
Fig. 6. Effect of CO₂ emission tax on water cost.

Fig. 7. Effect of panels cost on water cost.

expected from water cost per cubic meter from the PV–MVC to show higher sensitivity to changes in power-related costs including electric power, CO₂ emission tax and installed panels cost. This expectation is confirmed from the results shown in Table 12 where the values given represent the slopes of the lines drawn in Figs. 4–7.

Since it is assumed here that both plants have got identical product capacities and number of labors with the same salaries, the additional cost per cubic meter for any incremental change in labor payment will be the same in both plants. This is clear from Table 12 and the parallel lines in Fig. 4. However, at a monthly payment of \$1000, calculations for the RO and MVC plants give water costs as 3.12 and 6.6 \$/m³ respectively. If the payment is doubled, water costs will become 4.28 and 7.88 \$/m³, giving a percent increase of 37.2% and 17.7% to the initial costs, respectively. This means that, for the same incremental increase in labor payment, the figure representing water cost from the RO plant grows faster than its counterpart at the MVC plant.

6. Conclusions

A techno-economic analysis has been presented for two grid-connected PV–RO and PV–MVC desalination units with a capacity of a 100 m³/d. The two systems are aimed to produce freshwater from seawater for small isolated communities at remote areas in the UAE.

1. Design calculations reconfirmed the fact that seawater RO technology is significantly more energy efficient than MVC technology where for the first, the specific energy consumption came to be 6.45 kWh/\$/m³ against 15.7 kWh/\$/m³ for the latter. This gap could have been narrowed if the MVC unit had been designed for a smaller saturation temperature difference across the evaporator tube wall than the value assumed in this work, 3.5°C. In any case, a smaller driving force for heat transfer will result in a larger heat transfer area and larger dimensions of the evaporator.

2. Energy efficiency of the RO technology reflected itself in the lower specific costs of power-related operational items, e.g., cost of power from the grid, installed cost of solar panels and CO₂ emission tax. Accordingly, for the set of data given here, the RO option proved to be more cost effective and economically feasible than the MVC option, where the RO system gave a total water cost, including capital amortization plus operation and main-

tenance, of 3.7 \$/m³ vs. 7.29 \$/m³ in the case of the MVC system.

References

- [1] M. Darwish, Thermal analysis of vapor compression desalination system. *Desalination*, 69 (1988) 275–295.
- [2] F. Al-Juwayhel, H. El-Dessouky and H. Ettouney, Analysis of single-effect evaporator desalination systems combined with vapor compression heat pumps. *Desalination*, 114 (1997) 253–275.
- [3] H. Ettouney, H. El-Dessouky and Y. Al-Roumi, Analysis of mechanical vapor compression desalination process. *Intern. J. Energy Res.*, 23 (1999) 431–451.
- [4] M. Darwish, K. Fathallah and M. Ghazi, Thermodynamic analysis of vapor compression desalination system, Proc. 7th International Symposium on Fresh Water from the Sea, 1 (1980) 317–326.
- [5] B. Richards and I. Schafer, Design considerations for a solar-powered desalination system for remote communities in Australia. *Desalination*, 144 (2002) 193–199.
- [6] S. Avlonitis, K. Kouroumbas and N. Vlachakis, Energy consumption and membrane replacement cost for seawater RO desalination plants. *Desalination*, 157 (2003) 151–158.
- [7] A. Hafez and S. El- Manharawy, Economics of seawater RO desalination in the Red Sea region, Egypt. Part 1. A case study. *Desalination*, 153 (2003) 335–347.
- [8] Honda Worldwide, Honda to mass produce next-generation thin film solar cell. <http://world.honda.com/news/2005/c051219.html>, 2005.
- [9] G. Fiorenza, V. Sharma and G. Braccio, Techno-economic evaluation of a solar powered water desalination plant. *Energy Conv. Manage.*, 44 (2003) 2217–2240.
- [10] Z. Al Suleimani and V. Nair, Desalination by solar-powered reverse osmosis in a remote area of the Sultanate of Oman. *Appl. Energy*, 65 (2000) 367–380.
- [11] M. Tomson and D. Infield, A photovoltaic-powered seawater reverse-osmosis system without batteries. *Desalination*, 153 (2002) 1–8.
- [12] M. Thomson, J. Gwillim, A. Rowbottom, I. Draisey and M. Miranda, Batteryless photovoltaic reverse osmosis. *Desalination System*, S/P2/00305/REP, ETSU, DTI, UK.
- [13] United Nations, Economic and Social Commission for Western Asia, Water desalination technologies in the ESCWA member countries. New York, <http://www.escwa.org.lb/information/publications/edit/upload/tech-01-3-e.pdf>, 2001.
- [14] A. Helal and S. Al-Malek, Design of a solar-assisted mechanical vapor compression (MVC) desalination unit for remote areas in the United Arab Emirates, *Desalination*, 197 (2006) 273–300.
- [15] S. Avlonitis, G. Sakellariopoulos and W. Hanbury, Optimal design of spiral wound modules: an analytical method. *Trans IChemE*, 73 (1995) 575–581.
- [16] T. Markvart, *Solar Electricity*, Wiley, New York, 2000.
- [17] M. Marcoveccio, P. Aguirre and N. Scenna, Global optimal design of reverse osmosis networks for seawater desalination: Modeling and algorithm. *Desalination*, 184 (2005) 259–271.
- [18] A. Helal, S. Al-Malek and E. Al-Katheeri, Economic feasibility of alternative designs of a PV–RO desalination unit for remote areas in The United Arab Emirates, Conference on Desalination and the Environment, European Desalination Society and Center for Research and Technology Hellas (CERTH), Sani Resort, Halkidiki, Greece, 2007.
- [19] J.M. Veza, Mechanical vapor compression desalination plants – A case study, *Desalination*, 101 (1995) 1–10.